Noname manuscript No.
(will be inserted by the editor)

Accurate Time Series Prediction in Reduced Stochastic Epidemic Models

Lora Billings · **Eric Forgoston** · **Ira B. Schwartz**

Received: date / Accepted: date

Abstract We consider a stochastic Susceptible-Exposed-Infected-Recovered (SEIR) epidemiological model. Through the use of a normal form coordinate transform, we are able to analytically derive the stochastic center manifold along with the associated, reduced set of stochastic evolution equations. The transformation correctly projects both the dynamics and the noise onto the center manifold. Therefore, the solution of this reduced stochastic dynamical system yields excellent agreement, both in amplitude and phase, with the solution of the original stochastic system for a temporal scale that is orders of magnitude longer than the typical relaxation time. This new method allows for improved time series prediction of the number of infectious cases when modeling the spread of disease in a population. Numerical solutions of the fluctuations of the SEIR model are considered in the infinite population limit using a Langevin equation approach, as well as in a finite population simulated as a Markov process.

Keywords Epidemiology · Stochastic dynamical systems · Center manifold reduction

PACS 87.23.Cc · 05.45.-a · 05.10.Gg

1 Introduction

The interaction between deterministic and stochastic effects in population dynamics has played, and continues to play, an important role in the modeling of infectious diseases. The mechanistic modeling side of population dynamics is well-known and established [1; 4].

Eric Forgoston
Nonlinear Dynamical Systems Section, Plasma Physics Division, Code 6792, U.S. Naval Research Laboratory, Washington, DC 20375, USA
E-mail: eric.forgoston.ctr@nrl.navy.mil

Lora Billings
Department of Mathematical Sciences, Montclair State University, 1 Normal Avenue, Montclair, NJ 07043
E-mail: billingsl@mail.montclair.edu

Ira B. Schwartz
Nonlinear Dynamical Systems Section, Plasma Physics Division, Code 6792, U.S. Naval Research Laboratory, Washington, DC 20375, USA
E-mail: ira.schwartz@nrl.navy.mil

These models typically are assumed to be useful for infinitely large, homogeneous populations, and arise from the mean field analysis of probabilistic models. On the other hand, when one considers finite populations, random interactions give rise to internal noise effects, which may introduce new dynamics. Stochastic effects are quite prominent in finite populations, which can range from ecological dynamics [17] to childhood epidemics in cities [22; 26]. For homogeneous populations with seasonal forcing, noise also comes into play in the prediction of large outbreaks [24; 5; 30]. Specifically, external random perturbations change the probabilistic prediction of epidemic outbreaks as well as its control [28].

When geometric structure is applied to the population, the interactions are modeled as a network [23; 19], and therefore, even mean field approximations may be quite high-dimensional. Many types of static networks which support epidemics have been considered. Some examples include small world networks [31], hierarchical networks [33], and transportation networks of patch models [11]. In addition, the fluctuation of epidemics on adaptive networks,where the wiring between nodes changes in response to the node information, has been examined [29]. In adaptive network models, even the mean field can be high-dimensional, since nodes and links evolve in time and must be approximated as an additional set of ordinary differential equations.

Another aspect of epidemic models which is often of interest involves the inclusion of a time delay. The delay term makes the analysis significantly more complicated. However, it is possible to approximate the delay by creating a cascade consisting of a large number of compartments [18]. For example, one could simulate the delay associated with a disease exposure time with several hundred "exposed" compartments.

These model examples are just a few of the types of very high-dimensional models that are currently of interest. As a result of the high-dimensionality, there is much computation involved, and the analysis is quite difficult. In particular, real-time computation is not currently possible. However, there are usually many time scales that are well-separated when considering such high-dimensional problems. In the presence of well-separated time scales, a model reduction method is needed to examine the dynamics on a lower-dimensional space. It is known that deterministic model reduction methods may not work well in the stochastic realm, which includes epidemic models [15]. The purpose of this article is to examine a method of nonlinear, stochastic projection so that the deterministic and stochastic dynamics interact correctly on the lower-dimensional manifold and predict correctly the dynamics when compared to the full system. Because the noise affects the timing of outbreaks, it is essential to produce a low-dimensional system which captures the correct timing of the outbreaks as well as the amplitude and phase of any recurrent behavior.

We will demonstrate that our stochastic model reduction method properly captures the initial disease outbreak and continues to accurately predict the outbreaks for time scales which are orders of magnitude longer than the typical relaxation time. Furthermore, in practice, real disease data includes only the number of infectives. Our method allows us to predict the number of exposed people based on the observed number of infected people.

For stochastic model reduction, there exist several potential methods for general problems. For a system with certain spectral requirements, the existence of a stochastic center manifold was proven in [8]. Non-rigorous stochastic normal form analysis (which leads to the stochastic center manifold) was performed in [12; 16; 20; 21]. Rigorous theoretical analysis of normal form coordinate transformations for stochastic center manifold reduction was developed in [2; 3]. Later, another method of stochastic normal form reduction was developed [25], in which any anticipatory convolutions (integrals into the future of the noise processes) that appeared in the slow modes were removed. Since this latter analysis makes

the construction of the stochastic normal form coordinate transform more transparent, we use this method to derive the reduced stochastic center manifold equation.

Figure 1 shows a schematic demonstrating our approach to the problem. We consider a high-dimensional system along with its corresponding low-dimensional system. In this article, two types of low-dimensional system are discussed: a reduced system based on deterministic center manifold analysis and a reduced system based on a stochastic normal form coordinate transform. Regardless of the type of low-dimensional system being considered, a common noise is injected into both the high-dimensional and low-dimensional models, and an analysis of the solutions found using the high and low-dimensional systems is performed.

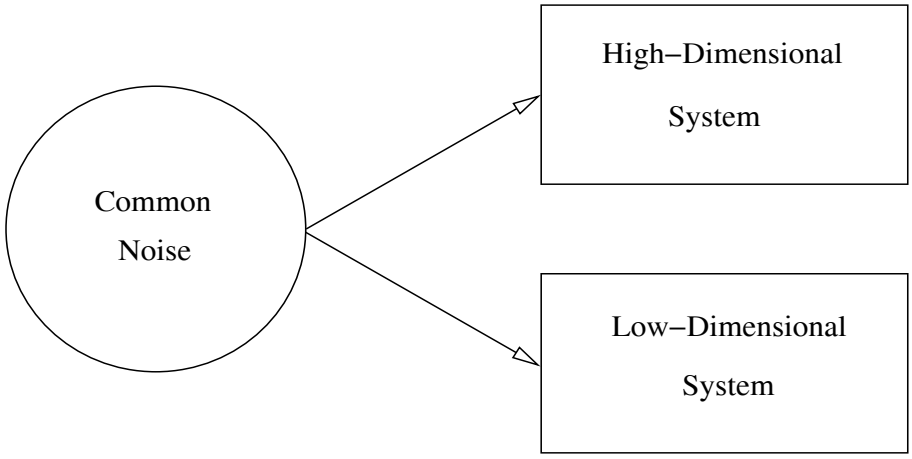

Fig. 1 Schematic demonstrating the injection of a common noise into both the high-dimensional system and its associated low-dimensional system.

In this article, as a first study of a high-dimensional system, we consider the Susceptible-Exposed-Infected-Recovered (SEIR) epidemiological model with stochastic forcing. As previously mentioned, we could easily consider a SEIR-type model where the exposed class was modeled using hundreds of compartments. Since the analysis is similar, we consider the simpler standard SEIR model to demonstrate the power of our method. Section 2 provides a complete description of this model. Section 3 describes how to transform the deterministic SEIR system to a new system that satisfies the spectral requirements needed to apply the center manifold theory. After the theory is used to find the evolution equations that describe the dynamics on the center manifold, we show in Sec. 4 how the reduced model that is found using the deterministic result incorrectly projects the noise onto the center manifold. Section 5 demonstrates the use of a stochastic normal form coordinate transform to correctly project the noise onto the stochastic center manifold, and the conclusions and discussion are contained in Sec. 6.

2 The SEIR model for epidemics

We begin by describing the stochastic version of the SEIR model found in [27]. We assume that a given population may be divided into the following four classes which evolve in time:

1. Susceptible class, $s(t)$, consists of those individuals who may contract the disease.
2. Exposed class, $e(t)$, consists of those individuals who have been infected by the disease but are not yet infectious.
3. Infectious class, $i(t)$, consists of those individuals who are capable of transmitting the disease to susceptible individuals.
4. Recovered class, $r(t)$, consists of those individuals who are immune to the disease.

Furthermore, we assume that the total population size, denoted as N, is constant and can be normalized to $S(t)+E(t)+I(t)+R(t)=1$, where $S(t)=s(t)/N$, $E(t)=e(t)/N$, $I(t)=i(t)/N$, and $R(t)=r(t)/N$. Therefore, the population class variables S, E, I, and R represent fractions of the total population. The governing equations for the stochastic SEIR model are given as

$$\dot{S}(t) = \mu - \beta I(t)S(t) - \mu S(t) + \sigma_1\phi_1(t), \tag{1a}$$
$$\dot{E}(t) = \beta I(t)S(t) - (\alpha+\mu)E(t) + \sigma_2\phi_2(t), \tag{1b}$$
$$\dot{I}(t) = \alpha E(t) - (\gamma+\mu)I(t) + \sigma_3\phi_3(t), \tag{1c}$$
$$\dot{R}(t) = \gamma I(t) - \mu R(t) + \sigma_4\phi_4(t), \tag{1d}$$

where σ_i is the standard deviation of the noise intensity $D_i=\sigma_i^2/2$. Each of the noise terms, ϕ_i, describes a stochastic, Gaussian white force that is characterized by the following correlation functions:

$$\langle\phi_i(t)\rangle = 0, \tag{2a}$$
$$\langle\phi_i(t)\phi_j(t')\rangle = \delta(t-t')\delta_{ij}. \tag{2b}$$

Additionally, μ represents a constant birth and death rate, β is the contact rate, α is the rate of infection, so that $1/\alpha$ is the mean latency period, and γ is the rate of recovery, so that $1/\gamma$ is the mean infectious period. Although the contact rate β could be given by a time-dependent function (e.g. due to seasonal fluctuations), for simplicity, we assume β to be constant. Throughout this article, we use the following parameter values: $\mu=0.02(\text{year})^{-1}$, $\beta=1575.0(\text{year})^{-1}$, $\alpha=1/0.0279(\text{year})^{-1}$, and $\gamma=1/0.01(\text{year})^{-1}$. Disease parameters correspond to typical measles values [27; 6]. Note that any other biologically meaningful parameters may be used as long as the basic reproductive rate $R_0>1$.

As a first approximation of stochastic effects, we have considered additive noise. This type of noise may result from migration into and away from the population being considered [9]. Since it is difficult to estimate fluctuating migration rates [7], it is appropriate to treat migration as an arbitrary external noise source. Also, fluctuations in the birth rate manifest itself as additive noise. Furthermore, as we are not interested in extinction events in this article, it is not necessary to use multiplicative noise. In general, for the problem considered here, it is possible that a rare event in the tail of the noise distribution may cause one or more of the S, E, and I components of the solution to become negative. In this article, we will always assume that the noise is sufficiently small so that a solution remains positive for a long enough time to gather sufficient statistics. Even though it is difficult to accurately estimate the appropriate noise level from real data, our choices of noise intensity lie within the huge

confidence intervals computed in [7]. The case for multiplicative noise will be considered in a separate paper.

Although $S+E+I+R=1$ in the deterministic system, one should note that the dynamics of the stochastic SEIR system will not necessarily have all of the components sum to unity. However, since the noise has zero mean, the total population will remain close to unity on average. Therefore, we assume that the dynamics are sufficiently described by Eqs. (1a)-(1c). It should be noted that even if $E(t)+I(t)=0$ for some t, the noise allows for the reemergence of the epidemic.

3 Deterministic center manifold analysis

One way to reduce the dimension of a system of equations is through the use of deterministic center manifold theory. In general, a nonlinear vector field can be transformed so that the linear part of the vector field has block diagonal form where the first matrix block has eigenvalues with positive real part, the second matrix block has eigenvalues with negative real part, and the third matrix block has eigenvalues with zero real part. These blocks are associated respectively with the unstable eigenspace, the stable eigenspace, and the center eigenspace. If we suppose that there are no eigenvalues with positive real part, then orbits will rapidly decay to the center eigenspace.

Equations (1a)-(1c) can not be written in block diagonal form with one block containing eigenvalues with negative real part and the other block containing eigenvalues with zero real part. Therefore, we must transform Eqs. (1a)-(1c) to a new system of equations that has the spectral structure that is needed to apply center manifold theory. The theory will allow us to find an invariant center manifold passing through the fixed point to which we can restrict the transformed system. Details regarding the transformation can be found in Sec. 3.1, and the computation of the center manifold can be found in Sec. 3.2.

3.1 Transformation of the SEIR model

Our analysis begins by considering the governing equations for the stochastic SEIR model given by Eqs. (1a)-(1c). We neglect the $\sigma_i\phi_i(t)$ terms in Eqs. (1a)-(1c) so that we are considering the deterministic SEIR system. This deterministic system has two fixed points. The first is given as

$$(S_e,E_e,I_e)=(1,0,0), \tag{3}$$

and corresponds to a disease free, or extinct, equilibrium state. The second corresponds to an endemic state and is given as

$$(S_0,E_0,I_0)=\left(\frac{(\gamma+\mu)(\alpha+\mu)}{\beta\alpha},\frac{\mu}{\alpha+\mu}-\frac{\mu(\gamma+\mu)}{\alpha\beta},\frac{\mu\alpha}{(\gamma+\mu)(\alpha+\mu)}-\frac{\mu}{\beta}\right). \tag{4}$$

To ease the analysis, we define a new set of variables, $\bar{S}$, $\bar{E}$, and $\bar{I}$, as $\bar{S}(t)=S(t)-S_0$, $\bar{E}(t)=E(t)-E_0$, and $\bar{I}(t)=I(t)-I_0$. These new variables are substituted into Eqs. (1a)-(1c).

Then, treating μ as a small parameter, we rescale time by letting $t=\mu\tau$. We may then introduce the following rescaled parameters: $\alpha=\alpha_0/\mu$ and $\gamma=\gamma_0/\mu$, where α_0 and γ_0 are $\mathcal{O}(1)$. The inclusion of the parameter μ as a new state variable means that the terms in our rescaled system which contain μ are now nonlinear terms. Furthermore, the system

is augmented with the auxiliary equation $\frac{d\mu}{d\tau} = 0$. The addition of this auxiliary equation contributes an extra simple zero eigenvalue to the system and adds one new center direction that has trivial dynamics. The shifted and rescaled, augmented system of equations is given as follows:

$$\frac{d\bar{S}}{d\tau} = -\beta\mu\bar{I}\bar{S} - \frac{(\alpha_0+\mu^2)(\gamma_0+\mu^2)}{\alpha_0}\bar{I} - \frac{\alpha_0\mu^3\beta}{(\alpha_0+\mu^2)(\gamma_0+\mu^2)}\bar{S}, \tag{5a}$$

$$\frac{d\bar{E}}{d\tau} = \beta\mu\bar{I}\bar{S} + \frac{(\alpha_0+\mu^2)(\gamma_0+\mu^2)}{\alpha_0}\bar{I} + \frac{\mu^2[\alpha_0\beta\mu - (\alpha_0+\mu^2)(\gamma_0+\mu^2)]}{(\alpha_0+\mu^2)(\gamma_0+\mu^2)}\bar{S} - (\alpha_0+\mu^2)\bar{E}, \tag{5b}$$

$$\frac{d\bar{I}}{d\tau} = \alpha_0\bar{E} - (\gamma_0+\mu^2)\bar{I}, \tag{5c}$$

$$\frac{d\mu}{d\tau} = 0, \tag{5d}$$

where the endemic fixed point is now located at the origin.

The Jacobian of Eqs. (5a)-(5d) is computed to zeroth-order in μ and is evaluated at the origin. Ignoring the μ components, the Jacobian has only two linearly independent eigenvectors. Therefore, the Jacobian is not diagonalizable. However, it is possible to transform Eqs. (5a)-(5c) to a block diagonal form with the eigenvalue structure that is needed to use center manifold theory. We use a transformation matrix, $\mathbf{P}$, consisting of the two linearly independent eigenvectors of the Jacobian along with a third vector chosen to be linearly independent. There are many choices for this third vector; our choice is predicated on keeping the vector as simple as possible. This transformation matrix can be found in Appendix A. Using the fact that $(\bar{S},\bar{E},\bar{I})^T = \mathbf{P}\cdot(U,V,W)^T$, then the transformation matrix leads to the following definition of new variables, U, V, and W:

$$U = \frac{-\gamma_0}{\alpha_0+\gamma_0}\bar{E}, \tag{6a}$$

$$V = \bar{S} + \frac{\gamma_0}{\alpha_0+\gamma_0}\bar{E}, \tag{6b}$$

$$W = \bar{I} + \bar{E}. \tag{6c}$$

The application of the transformation matrix to Eqs. (5a)-(5c) leads to the following transformed evolution equations:

$$\frac{dU}{d\tau} = -\alpha_0 U + \frac{\mu^2(\gamma_0 V - \alpha_0 U)}{\alpha_0+\gamma_0} - \frac{\left(\gamma_0+\mu^2\right)\left(\alpha_0+\mu^2\right)\left[(\alpha_0+\gamma_0)U+\gamma_0 W\right]}{\alpha_0(\alpha_0+\gamma_0)} - \frac{\mu\beta}{\alpha_0+\gamma_0}\left(\gamma_0 W + (\alpha_0+\gamma_0)U + \frac{\mu^2\alpha_0\gamma_0}{(\gamma_0+\mu^2)(\alpha_0+\mu^2)}\right)(U+V), \tag{7a}$$

$$\frac{dV}{d\tau} = \alpha_0 U - \frac{\mu^2(\gamma_0 V - \alpha_0 U)}{\alpha_0+\gamma_0} - \frac{\left(\gamma_0+\mu^2\right)\left(\alpha_0+\mu^2\right)\left[(\alpha_0+\gamma_0)U+\gamma_0 W\right]}{\gamma_0(\alpha_0+\gamma_0)} - \frac{\mu\beta\alpha_0}{\gamma_0(\alpha_0+\gamma_0)}\left(\gamma_0 W + (\alpha_0+\gamma_0)U + \frac{\mu^2\alpha_0\gamma_0}{(\gamma_0+\mu^2)(\alpha_0+\mu^2)}\right)(U+V), \tag{7b}$$

$$\frac{dW}{d\tau} = -\alpha_0 U - \left(\gamma_0+\mu^2\right)(U+W) + \frac{\left(\gamma_0+\mu^2\right)\left(\alpha_0+\mu^2\right)\left[(\alpha_0+\gamma_0)U+\gamma_0 W\right]}{\alpha_0\gamma_0} - \mu^2 V + \frac{\mu\beta}{\gamma_0}\left(\gamma_0 W + (\alpha_0+\gamma_0)U + \frac{\mu^2\alpha_0\gamma_0}{(\gamma_0+\mu^2)(\alpha_0+\mu^2)}\right)(U+V), \tag{7c}$$

$$\frac{d\mu}{d\tau} = 0. \tag{7d}$$

3.2 Center manifold equation

The Jacobian of Eqs. (7a)-(7d) to zeroth-order in μ and evaluated at the origin is

$$\left[\begin{array}{c|ccc} -(\alpha_0+\gamma_0) & 0 & -\frac{\gamma_0^2}{(\alpha_0+\gamma_0)} & 0 \\ \hline 0 & 0 & -\frac{\alpha_0\gamma_0}{(\alpha_0+\gamma_0)} & 0 \\ 0 & 0 & 0 & 0 \\ 0 & 0 & 0 & 0 \end{array}\right], \tag{8}$$

which shows that Eqs. (7a)-(7d) may be rewritten in the form

$$\frac{d\mathbf{x}}{d\tau} = \mathbf{A}\mathbf{x} + \mathbf{f}(\mathbf{x},\mathbf{y},\mu), \tag{9}$$

$$\frac{d\mathbf{y}}{d\tau} = \mathbf{B}\mathbf{y} + \mathbf{g}(\mathbf{x},\mathbf{y},\mu), \tag{10}$$

$$\frac{d\mu}{d\tau} = 0, \tag{11}$$

where $\mathbf{x} = (U)$, $\mathbf{y} = (V,W)$, $\mathbf{A}$ is a constant matrix with eigenvalues that have negative real parts, $\mathbf{B}$ is a constant matrix with eigenvalues that have zero real parts, and $\mathbf{f}$ and $\mathbf{g}$ are nonlinear functions in $\mathbf{x}$, $\mathbf{y}$ and μ. In particular,

$$\mathbf{A} = \left[-(\alpha_0+\gamma_0)\right], \qquad \mathbf{B} = \begin{bmatrix} 0 & -\frac{\alpha_0\gamma_0}{(\alpha_0+\gamma_0)} \\ 0 & 0 \end{bmatrix}. \tag{12}$$

Therefore, the system will rapidly collapse onto a lower-dimensional manifold given by center manifold theory [10]. Furthermore, since **x** is associated with **A** and **y** is associated with **B**, we know that the center manifold is given by

$$U = h(V,W,\mu), \tag{13}$$

where h is an unknown function.

Substitution of Eq. (13) into Eq. (7a) leads to the following center manifold condition:

$$\begin{aligned}
&\frac{\partial h(V,W,\mu)}{\partial V}\frac{dV}{d\tau} + \frac{\partial h(V,W,\mu)}{\partial W}\frac{dW}{d\tau} = -\alpha_0 h(V,W,\mu) + \frac{\mu^2\left[\gamma_0 V - \alpha_0 h(V,W,\mu)\right]}{\alpha_0+\gamma_0} - \\
&\frac{\left(\gamma_0+\mu^2\right)\left(\alpha_0+\mu^2\right)\left[\left(\alpha_0+\gamma_0\right)h(V,W,\mu)+\gamma_0 W\right]}{\alpha_0\left(\alpha_0+\gamma_0\right)} - \\
&\frac{\mu\beta}{\alpha_0+\gamma_0}\left(\gamma_0 W + \left(\alpha_0+\gamma_0\right)h(V,W,\mu) + \frac{\mu^2\alpha_0\gamma_0}{\left(\gamma_0+\mu^2\right)\left(\alpha_0+\mu^2\right)}\right)\left(h(V,W,\mu)+V\right).
\end{aligned} \tag{14}$$

In general, it is not possible to solve the center manifold condition for the unknown function, $h(V,W,\mu)$. Therefore, we perform the following Taylor series expansion of $h(V,W,\mu)$ in V, W, and μ:

$$\begin{aligned}
h(V,W,\mu) =& h_0 + h_2 V + h_3 W + h_\mu \mu + h_{22}V^2 + h_{23}VW + h_{33}W^2 + \\
& h_{\mu 2}\mu V + h_{\mu 3}\mu W + h_{\mu\mu}\mu^2 + \ldots,
\end{aligned} \tag{15}$$

where h_0, h_2, h_3, h_μ, ... are unknown coefficients that are found by substituting the Taylor series expansion into the center manifold condition and equating terms of the same order. By carrying out this procedure using a second-order Taylor series expansion of h, we have found the center manifold equation to be

$$U = -\frac{\gamma_0^2}{(\alpha_0+\gamma_0)^2}W + \mathcal{O}(\varepsilon^3), \tag{16}$$

where $\varepsilon = |(V,W,\mu)|$ so that ε provides a count of the number of V, W, and μ factors in any one term. Substitution of Eq. (16) into Eqs. (7b) and (7c) leads to the following reduced system of evolution equations which describe the dynamics on the center manifold:

$$\begin{aligned}
\frac{dV}{d\tau} =& -\frac{\mu^2\gamma_0{}^2\alpha_0 W}{(\alpha_0+\gamma_0)^3} - \frac{\mu^4\alpha_0 W}{(\alpha_0+\gamma_0)^2} - \frac{\gamma_0\mu^2 V}{\alpha_0+\gamma_0} - \frac{\left(\gamma_0+\mu^2\right)\alpha_0 W}{\alpha_0+\gamma_0} - \\
& \frac{\beta\alpha_0{}^2\mu}{(\alpha_0+\gamma_0)^2}\left(W + \frac{\mu^2(\alpha_0+\gamma_0)}{(\gamma_0+\mu^2)(\alpha_0+\mu^2)}\right)\left(V - \frac{\gamma_0{}^2 W}{(\alpha_0+\gamma_0)^2}\right),
\end{aligned} \tag{17a}$$

$$\begin{aligned}
\frac{dW}{d\tau} =& \frac{\mu^2\gamma_0{}^2 W}{(\alpha_0+\gamma_0)^2} + \frac{\mu^4 W}{\alpha_0+\gamma_0} - \mu^2 V + \\
& \frac{\beta\mu\alpha_0}{\alpha_0+\gamma_0}\left(W + \frac{\mu^2(\alpha_0+\gamma_0)}{(\gamma_0+\mu^2)(\alpha_0+\mu^2)}\right)\left(V - \frac{\gamma_0{}^2 W}{(\alpha_0+\gamma_0)^2}\right).
\end{aligned} \tag{17b}$$

4 Incorrect projection of the noise onto the stochastic center manifold

4.1 Transformation of the stochastic SEIR model

We now return to the stochastic SEIR system given by Eqs. (1a)-(1c). The shift of the fixed point to the origin will not have any effect on the noise terms, so that the stochastic version of the shifted equations will be

$$\dot{\bar{S}}(t) = -\beta\overline{IS} - \frac{(\alpha+\mu)(\gamma+\mu)}{\alpha}\bar{I} - \frac{\alpha\mu\beta}{(\alpha+\mu)(\gamma+\mu)}\bar{S} + \sigma_1\phi_1(t), \tag{18a}$$

$$\dot{\bar{E}}(t) = \beta\overline{IS} + \frac{(\alpha+\mu)(\gamma+\mu)}{\alpha}\bar{I} + \frac{\mu[\alpha\beta-(\alpha+\mu)(\gamma+\mu)]}{(\alpha+\mu)(\gamma+\mu)}\bar{S} - (\alpha+\mu)\bar{E} + \sigma_2\phi_2(t), \tag{18b}$$

$$\dot{\bar{I}}(t) = \alpha\bar{E} - (\gamma+\mu)\bar{I} + \sigma_3\phi_3(t). \tag{18c}$$

As Eqs. (18a)-(18c) are transformed using Eqs. (6a)-(6c), the $\alpha = \alpha_0/\mu$ scaling, the $\gamma = \gamma_0/\mu$ scaling, and the $t = \mu\tau$ time scaling, the noise also is scaled so that the stochastic, transformed equations are given by

$$\frac{dU}{d\tau} = -\alpha_0 U + \frac{\mu^2(\gamma_0 V - \alpha_0 U)}{\alpha_0+\gamma_0} - \frac{\left(\gamma_0+\mu^2\right)\left(\alpha_0+\mu^2\right)[(\alpha_0+\gamma_0)U+\gamma_0 W]}{\alpha_0(\alpha_0+\gamma_0)} - \frac{\mu\beta}{\alpha_0+\gamma_0}\left(\gamma_0 W + (\alpha_0+\gamma_0)U + \frac{\mu^2\alpha_0\gamma_0}{(\gamma_0+\mu^2)(\alpha_0+\mu^2)}\right)(U+V) + \sigma_4\phi_4, \tag{19a}$$

$$\frac{dV}{d\tau} = \alpha_0 U - \frac{\mu^2(\gamma_0 V - \alpha_0 U)}{\alpha_0+\gamma_0} - \frac{\left(\gamma_0+\mu^2\right)\left(\alpha_0+\mu^2\right)[(\alpha_0+\gamma_0)U+\gamma_0 W]}{\gamma_0(\alpha_0+\gamma_0)} - \frac{\mu\beta\alpha_0}{\gamma_0(\alpha_0+\gamma_0)}\left(\gamma_0 W + (\alpha_0+\gamma_0)U + \frac{\mu^2\alpha_0\gamma_0}{(\gamma_0+\mu^2)(\alpha_0+\mu^2)}\right)(U+V) + \sigma_5\phi_5, \tag{19b}$$

$$\frac{dW}{d\tau} = -\alpha_0 U - \left(\gamma_0+\mu^2\right)(U+W) + \frac{\left(\gamma_0+\mu^2\right)\left(\alpha_0+\mu^2\right)[(\alpha_0+\gamma_0)U+\gamma_0 W]}{\alpha_0\gamma_0} - \mu^2 V + \frac{\mu\beta}{\gamma_0}\left(\gamma_0 W + (\alpha_0+\gamma_0)U + \frac{\mu^2\alpha_0\gamma_0}{(\gamma_0+\mu^2)(\alpha_0+\mu^2)}\right)(U+V) + \sigma_6\phi_6, \tag{19c}$$

where

$$\sigma_4\phi_4 = -\frac{\mu\gamma_0}{\alpha_0+\gamma_0}\sigma_2\phi_2, \tag{20a}$$

$$\sigma_5\phi_5 = \mu\sigma_1\phi_1 + \frac{\mu\gamma_0}{\alpha_0+\gamma_0}\sigma_2\phi_2, \tag{20b}$$

$$\sigma_6\phi_6 = \mu\sigma_2\phi_2 + \mu\sigma_3\phi_3. \tag{20c}$$

The stochastic terms ϕ_4, ϕ_5, and ϕ_6 in Eqs. (19a)-(19c) are still additive, Gaussian noise processes. However, Eqs. (20a)-(20c) show how the transformation has acted on the original stochastic terms ϕ_1, ϕ_2, and ϕ_3 to create new noise processes which have a variance different from that of the original noise processes. Also note that we have suppressed the argument of ϕ_4, ϕ_5, and ϕ_6 in Eqs. (19a)-(19c). The time scaling means that these noise terms should be evaluated at $\mu\tau$.

The system of equations given by Eqs. (19a)-(20c) are an exact transformation of the system of equations given by Eqs. (1a)-(1c). We numerically integrate the original, stochastic system of the SEIR model [Eqs. (1a)-(1c)] along with the transformed, stochastic system

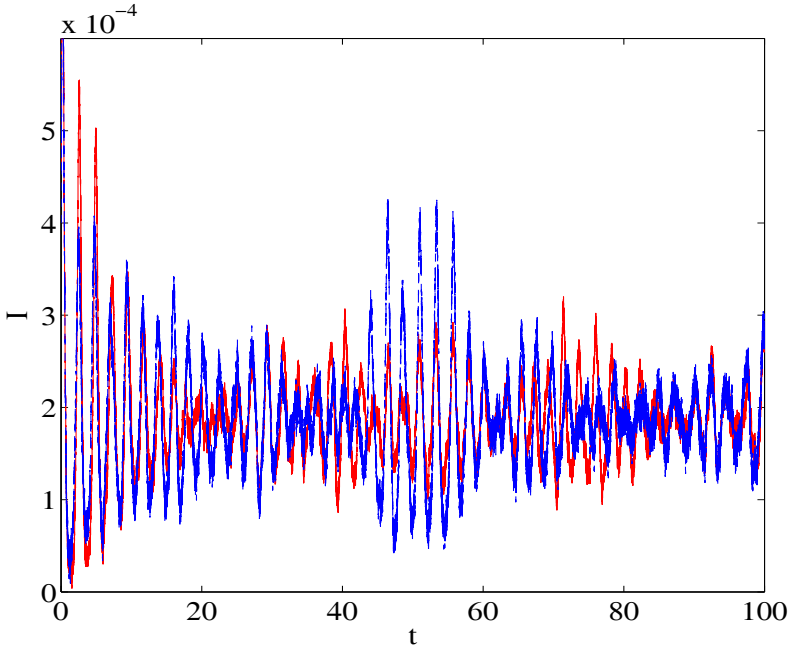

Fig. 2 (Color online) Time series of the fraction of the population that is infected with a disease, I, computed using the original, stochastic system of equations of the SEIR model [Eqs. (1a)-(1c)] (red, solid line), and computed using the transformed, stochastic system of equations of the SEIR model [Eqs. (19a)-(19c)] (blue, dashed line). The standard deviation of the noise intensity used in the simulation is $\sigma_i = 0.0005$, $i = 1,\ldots,6$.

[Eqs. (19a)-(19c)] using a stochastic fourth-order Runge-Kutta scheme with a constant time step size. The original system is solved for S, E, and I, while the transformed system is solved for U, V, and W. In the latter case, once the values of U, V, and W are known, we compute the values of $\bar{S}$, $\bar{E}$, and $\bar{I}$ using the transformation given by Eqs. (6a)-(6c). We shift $\bar{S}$, $\bar{E}$, and $\bar{I}$ respectively by S_0, E_0, and I_0 to find the values of S, E, and I.

Figure 2 compares the time series of the fraction of the population that is infected with a disease, I, computed using the original, stochastic system of equations of the SEIR model with the time series of I computed using the transformed, stochastic system of equations of the SEIR model.

Although the two time series shown in Fig. 2 generally agree very well, there is some discrepancy. This discrepancy is due to the fact that the noise processes $\sigma_4\phi 4$, $\sigma_5\phi_5$, and $\sigma_6\phi_6$ of the transformed system are new, independent noise processes with different variance than the $\sigma_1\phi_1$, $\sigma_2\phi_2$, and $\sigma_3\phi_3$ noise processes found in the original system. If we carefully take the noise realization from the original system, transform this noise using Eqs. (20a)-(20c), and use this realization to solve the transformed system, then the two solutions would be identical.

4.2 Reduction of the stochastic SEIR model

It is tempting to consider the reduced stochastic model found by substitution of Eq. (16) into Eqs. (19b) and (19c), so that one has the following stochastic evolution equations (that hopefully describe the dynamics on the stochastic center manifold):

$$\frac{dV}{d\tau} = -\frac{\mu^2\gamma_0{}^2\alpha_0 W}{(\alpha_0+\gamma_0)^3} - \frac{\mu^4\alpha_0 W}{(\alpha_0+\gamma_0)^2} - \frac{\gamma_0\mu^2 V}{\alpha_0+\gamma_0} - \frac{(\gamma_0+\mu^2)W\alpha_0}{\alpha_0+\gamma_0} - \frac{\beta\alpha_0{}^2\mu}{(\alpha_0+\gamma_0)^2}\left(W + \frac{\mu^2(\alpha_0+\gamma_0)}{(\gamma_0+\mu^2)(\alpha_0+\mu^2)}\right)\left(V - \frac{\gamma_0{}^2 W}{(\alpha_0+\gamma_0)^2}\right) + \sigma_5\phi_5, \tag{21a}$$

$$\frac{dW}{d\tau} = \frac{\mu^2\gamma_0{}^2 W}{(\alpha_0+\gamma_0)^2} + \frac{\mu^4 W}{\alpha_0+\gamma_0} - \mu^2 V + \frac{\beta\mu\alpha_0}{\alpha_0+\gamma_0}\left(W + \frac{\mu^2(\alpha_0+\gamma_0)}{(\gamma_0+\mu^2)(\alpha_0+\mu^2)}\right)\left(V - \frac{\gamma_0{}^2 W}{(\alpha_0+\gamma_0)^2}\right) + \sigma_6\phi_6. \tag{21b}$$

One should note that Eqs. (21a) and (21b) also can be found by naïvely adding the stochastic terms to the reduced system of evolution equations for the deterministic problem [Eqs. (17a) and (17b)]. This type of stochastic center manifold reduction has been done for the case of discrete noise [6]. Additionally, in many other fields (e.g. oceanography, solid mechanics, fluid mechanics), researchers have performed stochastic model reduction using a Karhunen-Loève expansion (principal component analysis, proper orthogonal decomposition) [13; 32]. However, this linear projection does not properly capture the nonlinear effects. Furthermore, one must subjectively choose the number of modes needed for the expansion. Therefore, even though the solution to the reduced model found using this technique may have the correct statistics, individual solution realizations will not agree with the original, complete solution.

We will show that Eqs. (21a) and (21b) do not contain the correct projection of the noise onto the center manifold. Therefore, when solving the reduced system, one does not obtain the correct solution. Such errors in stochastic epidemic modeling impact the prediction of disease outbreak when modeling the spread of a disease in a population.

Using the same numerical scheme previously described, we numerically integrate the complete, stochastic system of transformed equations of the SEIR model [Eqs. (19a)-(19c)] along with the reduced system of equations that is based on the deterministic center manifold with a replacement of the noise terms [Eqs. (21a) and (21b)]. The complete system is solved for U, V, and W, while the reduced system is solved for V and W. In the latter case, U is computed using the center manifold equation given by Eq. (16). Once the values of U, V, and W are known, we compute the values of S, E, and I using the transformation given by Eqs. (6a)-(6c). We shift $\bar{S}$, $\bar{E}$, and $\bar{I}$ respectively by S_0, E_0, and I_0 to find the values of S, E, and I.

Figures 3(a)-(b) compares the time series of the fraction of the population that is infected with a disease, I, computed using the complete, stochastic system of transformed equations of the SEIR model [Eqs. (19a)-(19c)] with the time series of I computed using the reduced system of equations of the SEIR model that is based on the deterministic center manifold with a replacement of the noise terms [Eqs. (21a) and (21b)]. Figure 3(a) shows the initial transients, while Fig. 3(b) shows the time series after the transients have decayed. One can see that solution computed using the reduced system quickly becomes out of phase with the solution of the complete system. Use of this reduced system would lead to an incorrect

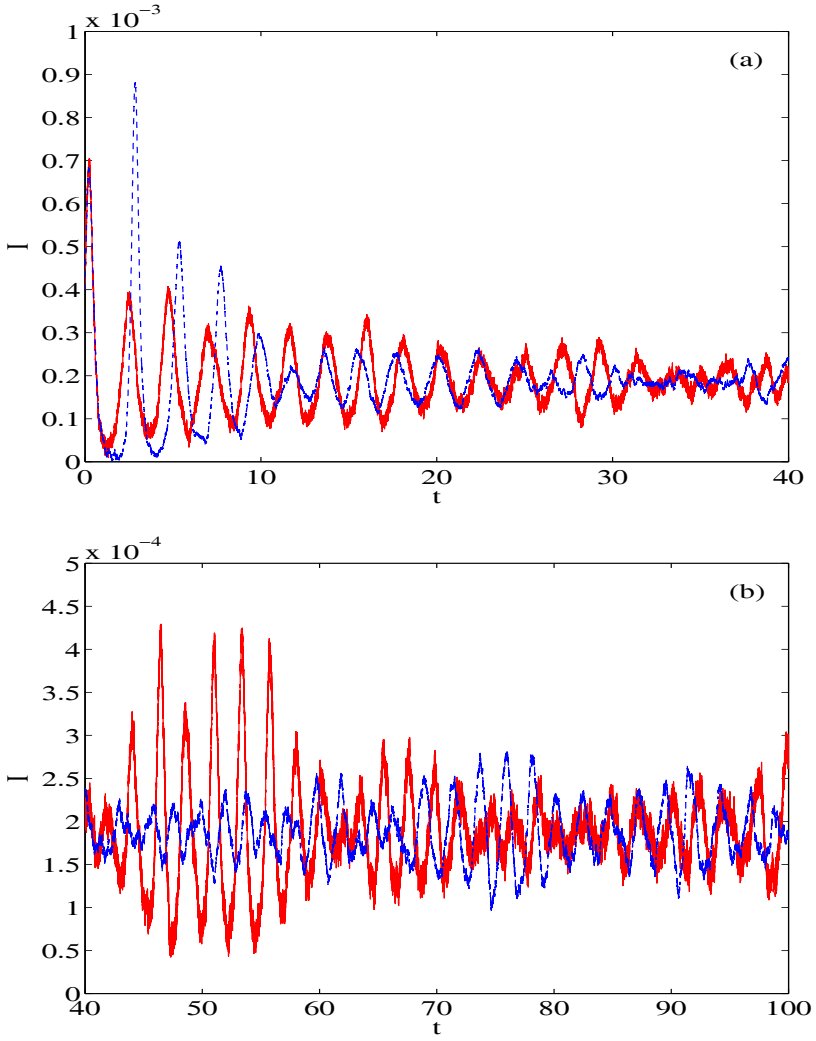

Fig. 3 (Color online) Time series of the fraction of the population that is infected with a disease, I, computed using the complete, stochastic system of transformed equations of the SEIR model [Eqs. (19a)-(19c)] (red, solid line), and computed using the reduced system of equations of the SEIR model that is based on the deterministic center manifold with a replacement of the noise terms [Eqs. (21a) and (21b)] (blue, dashed line). The standard deviation of the noise intensity used in the simulation is $\sigma_i = 0.0005$, $i = 4,5,6$. The time series is shown for (a) $t = 0$ to $t = 40$, and for (b) $t = 40$ to $t = 100$.

prediction of the initial disease outbreak. Additionally, the predicted amplitude of the initial outbreak would be incorrect. The poor agreement, both in phase and amplitude, between the two solutions continues for long periods of time as seen in Fig. 3(b). We also have computed the cross-correlation of the two time series shown in Fig. 3(a)-(b) to be approximately 0.34. Since the cross-correlation measures the similarity between the two time series, this low value quantitatively suggests poor agreement between the two solutions.

Using the same systems of transformed equations, we compute 140 years worth of time series for 500 realizations. Ignoring the first 40 years of transient solution, the data is used to create a histogram representing the probability density, p_{SI} of the S and I values. Figure 4(a) shows the histogram associated with the complete, stochastic system of transformed equations, while Fig. 4(b) shows the histogram associated with the reduced system of equations with a replacement of the noise terms. The color-bar values in Figs. 4(a)-(b) have been normalized by 10^{-3}.

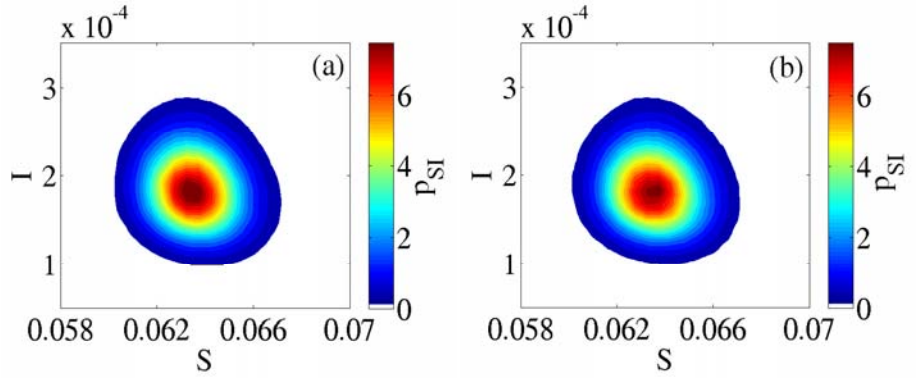

Fig. 4 (Color online) Histogram of probability density, p_{SI} of the S and I values found using (a) the complete, stochastic system of transformed equations for the SEIR model [Eqs. (19a)-(19c)], and (b) the reduced system of equations of the SEIR model that is based on the deterministic center manifold with a replacement of the noise terms [Eqs. (21a) and (21b)]. The histograms are created using 100 years worth of time series (starting with year 40) for 500 realizations, and the color-bar values have been normalized by 10^{-3}.

One can see by comparing Fig. 4(a) with Fig. 4(b) that the two probability distributions qualitatively look the same. It also is possible to compare the two distributions using a quantitative measure. The Kullback-Leibler divergence, or relative entropy, measures the difference between the two probability distributions as

$$d_{KL} = \sum_{i,j} P_{i,j} \left| \log\left(\frac{P_{i,j}}{Q_{i,j}}\right) \right|, \tag{22}$$

where $P_{i,j}$ refers to the (i,j)th component of the probability density found using the complete, stochastic system of transformed equations [Fig. 4(a)], and $Q_{i,j}$ refers to the (i,j)th component of the probability density found using the reduced system of equations [Fig. 4(b)]. In our numerical computation of the relative entropy, we have added 10^{-10} to each P_{ij} and Q_{ij}. This eliminates the possibility of having a $Q_{ij} = 0$ in the denominator of Eq. (22) and does not have much of an effect on the relative entropy.

If the two histograms were identical, then the relative entropy given by Eq. (22) would be $d_{KL} = 0$. The two histograms shown in Figs. 4(a)-(b) have a relative entropy of $d_{KL} = 0.0391$, which means that the two histograms, while not identical, are quantitatively very similar. However, one cannot rely entirely on the histograms alone to say that the solutions of the complete system and the reduced system agree. As we have seen in Figs. 3(a)-(b), the two solutions have differing amplitudes and are out of phase with one another. It is important to note that these features are not picked up by the histograms of Fig. 4.

5 Correct projection of the noise onto the stochastic center manifold

To project the noise correctly onto the center manifold, we will derive a normal form coordinate transform for the complete, stochastic system of transformed equations of the SEIR model given by Eqs. (19a)-(19c). The particular method we use to construct the normal form coordinate transform not only reduces the dimension of the dynamics, but also separates all of the fast processes from all of the slow processes [25]. This technique has been modified and applied to the large fluctuations of multiscale problems [15].

Many publications [16; 12; 20; 21] discuss the simplification of a stochastic dynamical system using a stochastic normal form transformation. In some of this work [12; 21], anticipative noise processes appeared in the normal form transformations, but these integrals of the noise process into the future were not dealt with rigorously.

Later, the rigorous, theoretical analysis needed to support normal form coordinate transforms was developed [3; 2]. The technical problem of the anticipative noise integrals also was dealt with rigorously in this work. Even later, another stochastic normal form transformation was developed [25]. This new method allows for the "[removal of] anticipation ... from the slow modes with the result that no anticipation is required after the fast transients decay"(Ref. [25], pp. 13). The removal of anticipation leads to a simplification of the normal form. Nonetheless, this simpler normal form retains its accuracy with the original stochastic system [25].

We shall use the method of [25] to simplify our stochastic dynamical system to one that emulates the long-term dynamics of the original system. The method involves five principles, which we recapitulate here for completeness:

1. Avoid unbounded, secular terms in both the transformation and the evolution equations to ensure a uniform asymptotic approximation.
2. Decouple all of the slow processes from the fast processes to ensure a valid long-term model.
3. Insist that the stochastic slow manifold is precisely the transformed fast processes coordinate being equal to zero.
4. To simplify matters, eliminate as many as possible of the terms in the evolution equations.
5. Try to remove all fast processes from the slow processes by avoiding as much as possible the fast time memory integrals in the evolution equations.

In practice, the original stochastic system of equations (which satisfies the necessary spectral requirements) in $(U,V,W)^T$ coordinates is transformed to a new $(Y,X_1,X_2)^T$ coordinate system using a near-identity stochastic coordinate transform as follows:

$$U = Y + \xi\left(Y,X_1,X_2,\tau\right), \tag{23a}$$

$$V = X_1 + \eta\left(Y,X_1,X_2,\tau\right), \tag{23b}$$

$$W = X_2 + \rho\left(Y,X_1,X_2,\tau\right), \tag{23c}$$

where the specific form of $\xi\left(Y,X_1,X_2,\tau\right)$, $\eta\left(Y,X_1,X_2,\tau\right)$, and $\rho\left(Y,X_1,X_2,\tau\right)$ is chosen to simplify the original system according to the five principles listed previously, and is found using an iterative procedure.

Several iterations lead to coordinate transforms for U, V, and W along with evolution equations describing the Y-dynamics, X_1-dynamics, and X_2-dynamics in the new coordinate system. The Y-dynamics have exponential decay to the $Y = 0$ slow manifold. Substitution

of $Y=0$ yields the following coordinate transforms:

$$\begin{aligned}U =&\sigma_4\mathscr{G}(\phi_4)+\frac{{\gamma_0}^2(\sigma_6\mathscr{G}(\phi_6)-X_2)}{(\alpha_0+\gamma_0)^2}+\mu\left[\frac{\gamma_0\beta[\sigma_5X_2\mathscr{G}(\phi_5)-X_1X_2+\sigma_6X_1\mathscr{G}(\phi_6)]}{(\alpha_0+\gamma_0)^2}-\right.\\&\left.\frac{\sigma_4\alpha_0\beta\gamma_0\mathscr{G}^2(\phi_4)[(\alpha_0+\gamma_0)X_1+\gamma_0X_2]}{(\alpha_0+\gamma_0)(\gamma_0+\mu^2)(\alpha_0+\mu^2)}\right]+\mu^2\left[\frac{\gamma_0[X_1\alpha_0-2X_2+2\sigma_6\mathscr{G}(\phi_6)]}{\alpha_0(\alpha_0+\gamma_0)}-\right.\\&\left.\frac{\sigma_4\mathscr{G}^2(\phi_4)}{(\gamma_0+\mu^2)(\alpha_0+\mu^2)}\left(\frac{2{\gamma_0}^3+{\alpha_0}^3}{\alpha_0+\gamma_0}+\frac{{\alpha_0}^2{\gamma_0}^2(\alpha_0+\gamma_0)}{(\gamma_0+\mu^2)(\alpha_0+\mu^2)}\right)-\frac{\sigma_5\gamma_0\mathscr{G}(\phi_5)}{(\alpha_0+\gamma_0)^2}\right]+\\&\mu^3\left[\frac{\beta[-X_1+\sigma_5\mathscr{G}(\phi_5)]}{(\alpha_0+\gamma_0)^2}-\frac{\sigma_4\beta\mathscr{G}^2(\phi_4)}{(\gamma_0+\mu^2)(\alpha_0+\mu^2)}\left(\frac{\alpha_0\gamma_0}{\alpha_0+\gamma_0}+\gamma_0X_2+X_1(\alpha_0+\gamma_0)\right)+\right.\\&\left.\frac{\beta(\sigma_6X_1\mathscr{G}(\phi_6)+\sigma_5X_2\mathscr{G}(\phi_5)-X_1X_2\alpha_0)}{\alpha_0(\alpha_0+\gamma_0)}\right]+\mathscr{O}(\mu^4),\end{aligned}\tag{24a}$$

$$\begin{aligned}V =&X_1+\mu\left[\frac{\sigma_4\alpha_0\beta X_1\mathscr{G}(\phi_4)}{\alpha_0+\gamma_0}+\frac{\sigma_4\alpha_0\beta X_2\mathscr{G}(\phi_4)}{(\alpha_0+\gamma_0)^2}\right]+\mu^2\left[\frac{\sigma_4\mathscr{G}(\phi_4)\left(\alpha_0^2+\alpha_0\gamma_0+\gamma_0^2\right)}{\gamma_0(\alpha_0+\gamma_0)^2}\right]+\\&\mu^3\left[\frac{\sigma_4\alpha_0\beta\mathscr{G}(\phi_4)}{\gamma_0(\alpha_0+\gamma_0)^2}+\frac{\sigma_4\beta X_2\mathscr{G}(\phi_4)}{\gamma_0(\alpha_0+\gamma_0)}+\frac{\sigma_4\beta X_1\mathscr{G}(\phi_4)}{\gamma_0^2}\right]+\mathscr{O}(\mu^4),\end{aligned}\tag{24b}$$

$$\begin{aligned}W =&X_2+\mu\left[-\frac{\sigma_4\beta X_1\mathscr{G}(\phi_4)}{\gamma_0}-\frac{\sigma_4\beta X_2\mathscr{G}(\phi_4)}{(\alpha_0+\gamma_0)}\right]+\mu^2\left[\frac{\sigma_4\mathscr{G}(\phi_4)\left(\alpha_0^2+\alpha_0\gamma_0+\gamma_0^2\right)}{\alpha_0\gamma_0(\alpha_0+\gamma_0)}\right]+\\&\mu^3\left[-\frac{\sigma_4\beta\mathscr{G}(\phi_4)}{\gamma_0(\alpha_0+\gamma_0)}-\frac{\sigma_4(\alpha_0+\gamma_0)\beta X_1\mathscr{G}(\phi_4)}{\alpha_0\gamma_0^2}-\frac{\sigma_4\beta X_2\mathscr{G}(\phi_4)}{\alpha_0\gamma_0}\right]+\mathscr{O}(\mu^4),\end{aligned}\tag{24c}$$

where

$$\mathscr{G}(\phi)=e^{-\aleph\tau}*\phi=\int_{-\infty}^{\tau}\exp[-\aleph\cdot(\tau-s)]\phi(s)ds,\quad \aleph=\frac{\alpha_0\gamma_0(\alpha_0+\gamma_0)}{(\alpha_0+\mu^2)(\gamma_0+\mu^2)},\tag{25}$$

and

$$\mathscr{G}^2(\phi)=e^{-\aleph\tau}*e^{-\aleph\tau}*\phi.\tag{26}$$

All of the stochastic terms in Eqs. (24a)-(24c) consist of integrals of the noise process into the past (convolutions), as given by Eqs. (25) and (26). Since these memory integrals are fast-time processes, and since we are interested in long-term slow processes, we ignore the memory integrals found in Eqs. (24a)-(24c) so that

$$\begin{aligned}U =&-\frac{\gamma_0^2X_2}{(\alpha_0+\gamma_0)^2}-\frac{\mu\beta X_1}{(\alpha_0+\gamma_0)}\left(\frac{\mu^2}{(\alpha_0+\gamma_0)}+\frac{\gamma_0X_2}{(\alpha_0+\gamma_0)}+\mu^2X_2\right)+\\&\frac{\mu^2\gamma_0}{(\alpha_0+\gamma_0)}\left(X_1-\frac{2X_2}{\alpha_0}\right),\end{aligned}\tag{27a}$$

$$V=X_1,\tag{27b}$$

$$W=X_2.\tag{27c}$$

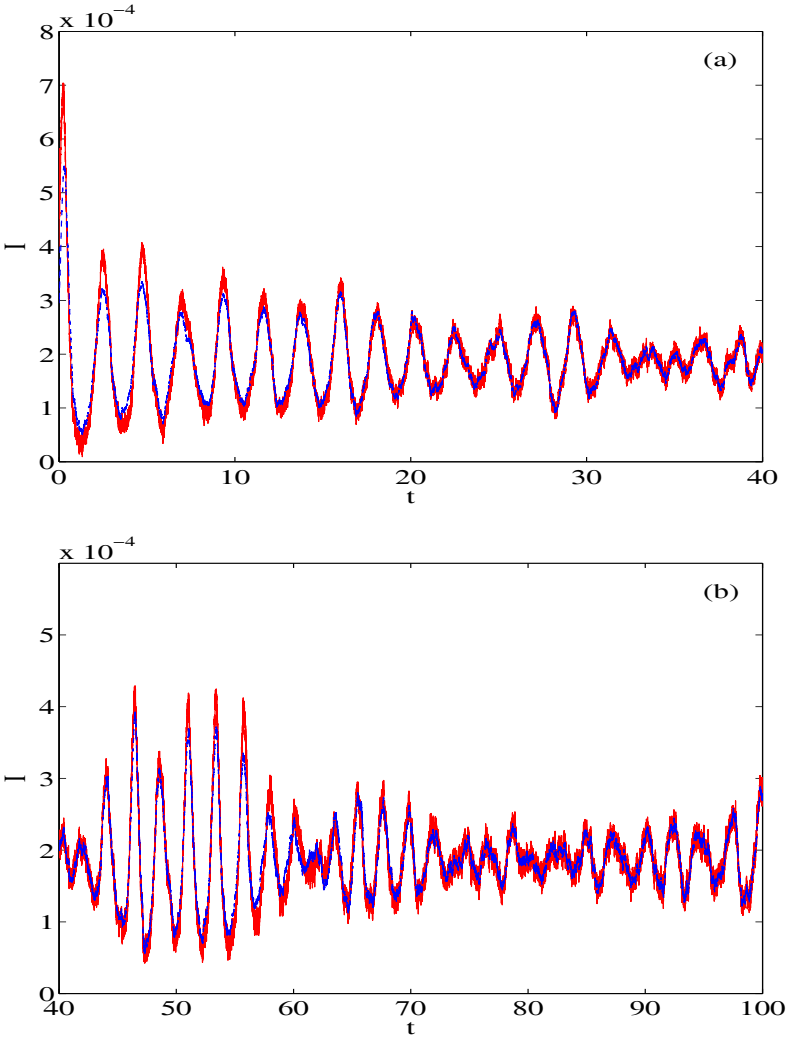

Fig. 5 (Color online) Time series of the fraction of the population that is infected with a disease, I, computed using the complete, stochastic system of transformed equations of the SEIR model [Eqs. (19a)-(19c)] (red, solid line), and computed using the reduced system of equations of the SEIR model that is found using the stochastic normal form coordinate transform [Eqs. (28a), (28b), (32a), and (32b)] (blue, dashed line). The standard deviation of the noise intensity used in the simulation is $\sigma_i = 0.0005$, $i = 4,5,6$. The time series is shown for (a) $t = 0$ to $t = 40$, and for (b) $t = 40$ to $t = 100$.

Note that Eq. (27a) is the deterministic center manifold equation, and at first-order, matches the center manifold equation that was found previously [Eq. (16)].

Substitution of $Y = 0$ and ignoring all multiplicative noise terms and memory integrals (so that we consider only first-order noise terms) leads to the following reduced system of

evolution equations on the center manifold:

$$\frac{dX_1}{d\tau} = F(X_1(\tau), X_2(\tau)), \tag{28a}$$

$$\frac{dX_2}{d\tau} = G(X_1(\tau), X_2(\tau)). \tag{28b}$$

The specific form of F and G in Eqs. (28a) and (28b) are complicated, and are therefore presented in Appendix B.

We numerically integrate the complete, stochastic system of transformed equations of the SEIR model [Eqs. (19a)-(19c)] along with the reduced system of equations that is found using the stochastic normal form coordinate transform [Eqs. (28a), (28b), (32a), and (32b)]. The complete system is solved for U, V, and W, while the reduced system is solved for $X_1 = V$ and $X_2 = W$. In the latter case, U is computed using the center manifold equation given by Eq. (27a). As before, once the values of U, V, and W are known, we compute the values of S, E , and I using the transformation given by Eqs. (6a)-(6c). We shift S, E, and I respectively by S_0, E_0, and I_0 to find the values of S, E, and I.

Figures 5(a)-(b) compares the time series of the fraction of the population that is infected with a disease, I, computed using the complete, stochastic system of transformed equations of the SEIR model [Eqs. (19a)-(19c)] with the time series of I computed using the reduced system of equations of the SEIR model that is found using the stochastic normal form coordinate transform [Eqs. (28a), (28b), (32a), and (32b)]. Figure 5(a) shows the initial transients, while Fig. 5(b) shows the time series after the transients have decayed. One can see that there is excellent agreement between the two solutions. The initial outbreak is successfully captured by the reduced system. Furthermore, Fig. 5(b) shows that the reduced system accurately predicts recurrent outbreaks for a time scale that is orders of magnitude longer than the relaxation time. The cross-correlation of the two time series shown in Fig. 3 is approximately 0.98, which quantitatively suggests there is excellent agreement between the two solutions.

Using the same systems of transformed equations, we compute 140 years worth of time series for 500 realizations. As before, we ignore the first 40 years worth of transient solution, and the data is used to create a histogram representing the probability density, p_{SI} of the S and I values. Figure 6(a) shows the histogram associated with the complete, stochastic system of transformed equations, while Fig. 6(b) shows the histogram associated with the reduced system of equations found using the normal form coordinate transform. The colorbar values in Figs. 6(a)-(b) have been normalized by 10^{-3}.

As we saw with Figs. 4(a)-(b), the probability distribution shown in Fig. 6(a) looks qualitatively the same as the probability distribution shown in Fig. 6(b). Using the Kullback-Leibler divergence given by Eq. (22), we have found that the two histograms shown in Figs. 6(a)-(b) have a relative entropy of $d_{KL} = 0.0953$. Since this value is close to zero, the two histograms are quantitatively very similar.

6 Conclusions and Discussion

We have considered the dynamics of an SEIR epidemiological model with stochastic forcing in the form of additive, Gaussian noise. We have presented two methods of model reduction, whereby the goal is to project both the noise and the dynamics onto the stochastic center manifold. The first method uses the deterministic center manifold found by neglecting

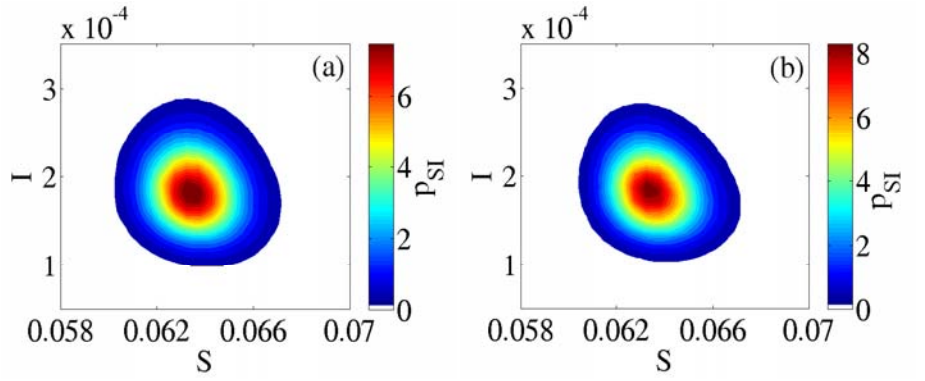

Fig. 6 (Color online) Histogram of probability density, p_{SI} of the S and I values found using (a) the complete, stochastic system of transformed equations for the SEIR model with mortality [Eqs. (19a)-(19c)], and (b) the reduced system of equations of the SEIR model with mortality that is found using the stochastic normal form coordinate transform [Eqs. (28a), (28b), (32a), and (32b)]. The histograms are created using 100 years worth of time series (starting with year 40) for 500 realizations, and the color-bar values have been normalized by 10^{-3}.

the stochastic terms in the governing equations, while the second method uses a stochastic normal form coordinate transform.

Since the original system of governing equations does not have the necessary spectral structure to employ either deterministic or stochastic center manifold theory, the system of equations has been transformed using an appropriate linear transformation coupled with appropriate parameter scaling. At this stage, the first method of model reduction can be performed by computing the deterministic center manifold equation. Substitution of this equation into the complete, stochastic system of transformed equations leads to a reduced system of stochastic evolution equations.

The solutions of the complete, stochastic system of transformed equations as well as the reduced system of equations were computed numerically. We have shown that the individual time series do not qualitatively nor quantitatively agree, because the noise has not been correctly projected onto the stochastic center manifold. However, by comparing histograms of the probability density, p_{SI} of the S and I values, we saw that there was very good agreement. This is caused by the fact that although the two solutions are out of phase with one another, their range of amplitude values are similar. The phase difference is not represented in the two histograms. This is a real drawback when trying to predict the timing of outbreaks, and leads to potential problems when considering epidemic control, such as the enhancement of disease extinction through random vaccine control [14].

To accurately project the noise onto the manifold, we derived a stochastic normal form coordinate transform for the complete, stochastic system of transformed equations. The coordinate transform is found using an iterative method, and contains integrals of the noise processes into the past. Since these integrals are fast time processes, and since we are interested in long-time slow behavior, they can be ignored. The numerical solution to this reduced system was compared with the solution to the original system, and we showed that there was excellent agreement, both qualitatively and quantitatively. As with the first method, the histograms of the probability density, p_{SI} of the S and I values agree very well.

It should be noted that the use of these two reduction methods is not constrained to problems in epidemiology, but rather may be used for many types of physical problems.

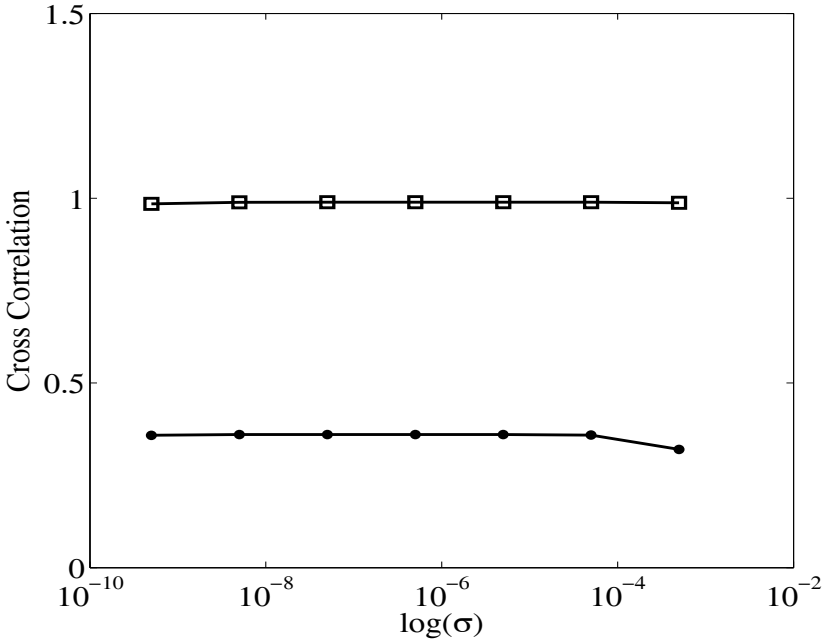

Fig. 7 Cross-correlation between time series found using the original, stochastic system of transformed equations and the reduced system of equations based on the deterministic center manifold ("circle" markers), and cross-correlation between time series found using the original, stochastic system of transformed equations and the reduced system of equations based on the stochastic normal form coordinate transform ("square" markers). The cross-correlation is computed using time series from $t = 800$ to $t = 1000$.

For some generic systems, such as the singularly perturbed, damped Duffing oscillator, either reduction method can be used since the terms in the normal form coordinate transform which lead to the average stochastic center manifold being different from the deterministic center manifold occur at very high order [15]. In other words, the average stochastic center manifold and deterministic center manifold are virtually identical. For the SEIR model considered in this article, there are terms at low order in the normal form transform which cause a significant difference between the average stochastic center manifold and the deterministic manifold. Therefore, as we have demonstrated, when working with the SEIR model, one must use the normal form coordinate transform method to correctly project the noise onto the center manifold.

In addition to computing the cross-correlation between the solution of the original system and the solutions of the two reduced systems for $\sigma_i = 0.0005$, we have computed the cross-correlation for the case of zero noise as well as for noise intensities ranging from $\sigma = 5.0 \times 10^{-10}$ to $\sigma = 5.0 \times 10^{-5}$. These cross-correlations were computed using time series from $t = 800$ to $t = 1000$. For the deterministic case (zero noise), the cross-correlation between the time series which were computed using the original system and the reduced system based on the deterministic center manifold is 1.0, since the agreement is perfect. The cross-correlation between the original system and the reduced system found using the stochastic normal form is also 1.0. Figure 7 shows the cross-correlation between the original system and the two reduced systems for various values of σ.

One can see in Fig. 7 that the solutions found using the reduced system based on the deterministic center manifold compare poorly with the original system at very low noise values. Furthermore, as the noise increases, the agreement between the two solutions gets worse. On the other hand, Fig. 7 shows that the solutions computed using the reduced system found using the normal form coordinate transform compare very well with the solutions to the original system across a wide range of small noise intensities.

It is worth pointing out that one might wish to replace the stochastic terms by deterministic, period functions of small amplitude. As an example, one could consider the following sinusoidal functions:

$$\sigma_1\phi_1 = \cos(10\pi\mu t)/8000, \tag{29a}$$

$$\sigma_2\phi_2 = \sin(4\pi\mu t)/8000, \tag{29b}$$

$$\sigma_3\phi_3 = \cos(10\pi\mu t)/8000, \tag{29c}$$

where $\sigma_4\phi_4$, $\sigma_5\phi_5$, and $\sigma_6\phi_6$ are given by Eqs. (20a)-(20c). Using Eqs. (29a)-(29c) or some other similar deterministic drive, the solution computed using the reduced system based on the deterministic center manifold analysis will agree perfectly with the solution computed using the complete system of equations. On the other hand, since the reduced system based on the normal form analysis was derived specifically for white noise, the transient solution found using this reduced system will not agree with the solution found using the complete system. It is possible to find a normal form coordinate transform for periodic forcing, but the normal form will be different than the one derived in this article for white noise.

Figures 8(a)-(b) compares the time series of the fraction of the population that is infected with a disease, I, computed using the complete system of transformed equations of the SEIR model [Eqs. (19a)-(19c)] with the time series of I computed using the reduced system of equations of the SEIR model that is found using the stochastic normal form coordinate transform [Eqs. (28a), (28b), (32a), and (32b)], but where the stochastic terms of both systems have been replaced by the deterministic terms given by Eqs. (29a)-(29c). Figure 8(a) shows the initial transients, while Fig. 8(b) shows a piece of the time series after the transients have decayed. One can see in Figs. 8(a)-(b) that although the two solutions eventually become relatively synchronized with one another, there is poor agreement, both in phase and amplitude, throughout the transient.

The solutions to the original system and both reduced systems are continuous solutions based on an infinite population assumption, and are found using Langevin equations having Gaussian noise. It is interesting to examine the effects of general noise by using a Markov simulation to compare solutions of the original and reduced systems.

The complete system in the original variables (see page 3) will evolve in time t in the following way:

transition	rate
$(s-1,e+1,i)$	$\beta si/N$
$(s,e-1,i+1)$	αe
$(s,e,i-1)$	γi
$(s+1,e,i)$	μN
$(s-1,e,i)$	μs
$(s,e-1,i)$	μe
$(s,e,i-1)$	μi

. (30)

Using a total population size of $N = 10$ million, we have performed a Markov simulation of the system. After completing the Markov simulation, we divided s, e, and i by N to find S, E, and I. Figure 9(a) shows a time series, after the transients have decayed, of the fraction

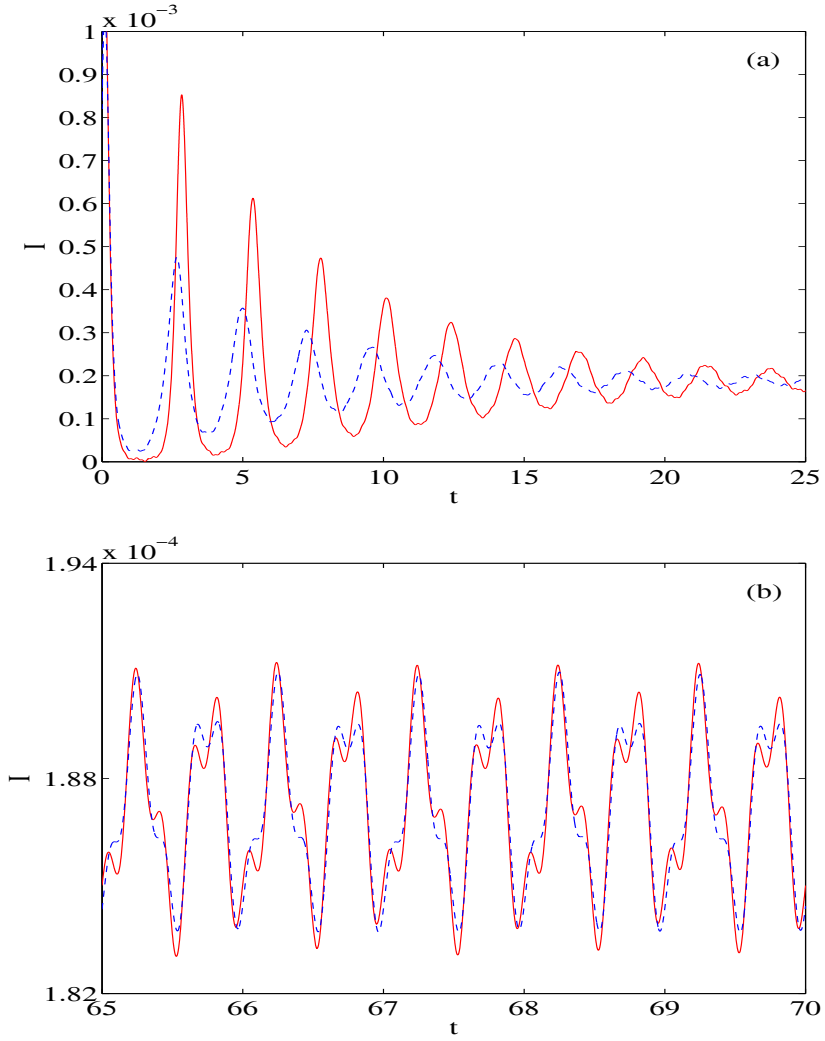

Fig. 8 (Color online) Time series of the fraction of the population that is infected with a disease, I, computed using the complete system of transformed equations of the SEIR model [Eqs. (19a)-(19c)] (red, solid line), and computed using the reduced system of equations of the SEIR model that is found using the normal form coordinate transform [Eqs. (28a), (28b), (32a), and (32b)] (blue, dashed line). The stochastic terms in both systems have been replaced by the deterministic terms given by Eqs. (29a)-(29b). The time series is shown from (a) $t = 0$ to $t = 25$, and from (b) $t = 65$ to $t = 70$.

of the population that is infected with a disease, I. The results reflect both the mean and the frequency of the deterministic system. Performing the simulation for 500 realizations allows us to create a histogram representing the probability density, p_{SI} of the S and I values. This histogram is shown in Fig. 9(b), and one can see that the probability density reflects the amplitude, which varies with the population size, of S and I. The color-bar values in Fig. 9(b) have been normalized by 10^{-4}

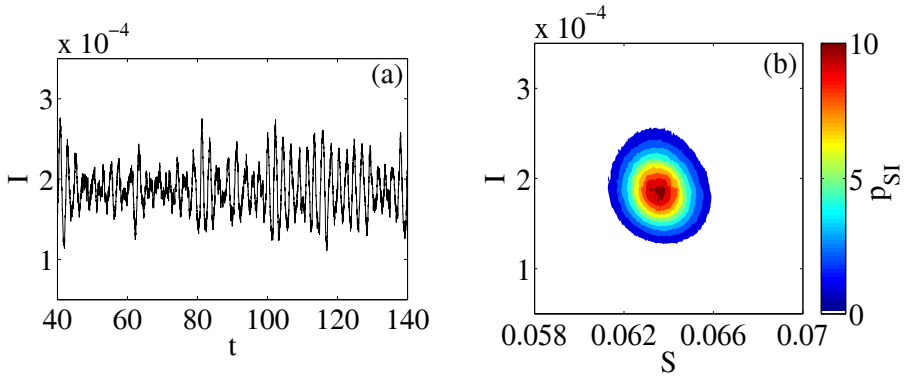

Fig. 9 (a) Time series of the fraction of the population that is infected with a disease, I, computed using a Markov simulation of the complete, original equations of the SEIR model [Eq. (30)], and (b) (color online) a histogram of probability density, p_{SI} of the S and I values found using a Markov simulation of Eq. (30). The histogram is created using 100 years worth of data (starting with year 40) for 500 realizations, and the color-bar values have been normalized by 10^{-4}.

The complete system in the transformed variables has the stable endemic equilibrium at the origin. To bound the dynamics to the first octant, we use the fact that $s \geq 0$, $e \geq 0$, and $i \geq 0$ to derive the appropriate inequalities for the transformed, discrete variables u, v, and w. These inequalities can be found in Appendix C as Eq. (33). These inequalities enable us to define new discrete variables Y_1, Y_2, and Y_3, given by Eqs. (34a)-(34c) in Appendix C.

In the Y_i variables, we define evolution relationships similar to those found in Eq. (30). The complete transformed system will evolve in time τ according to the transition and rates given by Eq. (35) in Appendix C.

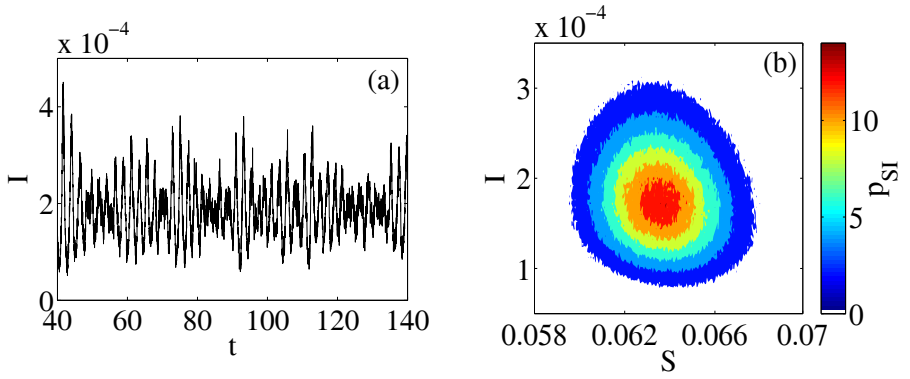

Fig. 10 (a) Time series of the fraction of the population that is infected with a disease, I, computed using a Markov simulation of the complete, transformed equations of the SEIR model [Eq. (35)], and (b) (color online) a histogram of probability density, p_{SI} of the S and I values found using a Markov simulation of Eq. (35). The histogram is created using 100 years worth of data (starting with year 40) for 500 realizations, and the color-bar values have been normalized by 10^{-4}.

After performing a Markov simulation of Eq. (35) with a population size of $N = 10$ million, we can compare the dynamics of the transformed system to the dynamics of the original

system by transforming the Y_i variables in the time series back to the original s, e, and i variables. Dividing by N yields S, E, and I. Figure 10(a) shows a time series, after the transients have decayed, of the fraction of the population that is infected with a disease, I. The mean and the frequency agree with those found from the Markov simulation of the original system. We have performed the simulation for 500 realizations, and a histogram representing the probability density, p_{SI} is shown in Fig. 10(b). The color-bar values in Fig. 10(b) have been normalized by 10^{-4}. One can see in Fig. 10(a) that the relative fluctuations of the I component has nearly doubled. While the fluctuation size was 0.152 for the original system, it is 0.310 for the transformed system. Additionally, the two histograms shown in Figs. 9(b) and 10(b) have a relative entropy of $d_{KL} = 0.9519$, which means they are not in agreement. Because the simulation of the stochastic dynamics in the complete system of transformed variables do not qualitatively (or quantitatively) resemble the original stochastic system, we cannot expect that the reduced system will agree with either the original or the transformed systems. Therefore, much care should be exercised when extending the model reduction results (which show outstanding agreement) derived for a specific type of noise in the limit of infinite population to finite populations with a more general type of noise.

In summary, we have presented a new method of stochastic model reduction that allows for dramatic improvement in time series prediction. The reduced model captures both the amplitude and phase accurately for a temporal scale that is many orders of magnitude longer than the typical relaxation time. Since sufficient statistics of disease data are limited due to short time series collection, the results presented here provide a potential method to properly model real, stochastic disease data in the time domain. Such long-term accuracy of the reduced model will allow for the application of effective control of a disease where phase differences between outbreak times and vaccine controls are important. Additionally, since our method is general, it may be applied to very high-dimensional epidemic models, such as those involving adaptive networks. From a dynamical systems viewpoint, the reduction method has the potential to accurately capture new, emergent dynamics as we increase the size of the random fluctuations. This could be a means to identify new noise-induced phenomena in generic stochastic systems.

Acknowledgments

We gratefully acknowledge support from the Office of Naval Research and the Army Research Office. E.F. is supported by a National Research Council Research Associateship, and L.B. is supported by ARO W911NF-06-1-0320.

A Transformation Matrix

$$\mathbf{P} = \begin{bmatrix} 1 & 1 & 0 \\ -\frac{\alpha_0+\gamma_0}{\gamma_0} & 0 & 0 \\ \frac{\alpha_0+\gamma_0}{\gamma_0} & 0 & 1 \end{bmatrix}. \tag{31}$$

B Reduced, stochastic SEIR model: Correct projection of the noise

The specific form of F and G in Eqs. (28a) and (28b) are given as follows:

$$
\begin{aligned}
F = &-\left[\alpha_0^2\gamma_0^3 X_2 + \frac{\mu\beta\alpha_0^2}{(\alpha_0+\gamma_0)}\gamma_0^2\left(-\frac{\gamma_0^2}{\alpha_0+\gamma_0}X_2^2 + \alpha_0 X_1 X_2\right) + \mu^2\left(\alpha_0\gamma_0^3 X_1 + \right.\right. \\
&\frac{\alpha_0\gamma_0^2\left(2\alpha_0^3+5\alpha_0^2\gamma_0+5\alpha_0\gamma_0^2+\gamma_0^3\right)}{(\alpha_0+\gamma_0)^2}X_2 - \frac{\alpha_0^2\beta^2\gamma_0^2}{(\alpha_0+\gamma_0)}X_1^2X_2 - \frac{\alpha_0^2\beta^2\gamma_0^3}{(\alpha_0+\gamma_0)^2}X_1X_2^2\Big) + \\
&\mu^3\left(\alpha_0^2\beta\gamma_0 X_1 - \frac{\alpha_0^2\beta\gamma_0^3}{(\alpha_0+\gamma_0)^2}X_2 + \frac{\alpha_0^2\beta\gamma_0^2}{(\alpha_0+\gamma_0)}X_1^2 - \frac{3\alpha_0\beta\gamma_0^3}{(\alpha_0+\gamma_0)}X_2^2 + \right. \\
&\left.\left.\frac{\alpha_0\beta\gamma_0\left(\alpha_0^3-\alpha_0^2\gamma_0-3\alpha_0\gamma_0^2-3\gamma_0^3\right)}{(\alpha_0+\gamma_0)^2}X_1X_2\right)\right] / \left[\gamma_0\left(\alpha_0+\gamma_0\right)\left(\alpha_0+\mu^2\right)\left(\gamma_0+\mu^2\right)\right] + \\
&\sigma_5\phi_5 - \frac{\mu^2(\alpha_0^2+\alpha_0\gamma_0+\gamma_0^2)}{(\alpha_0+\gamma_0)^3}\left(\frac{\sigma_4\alpha_0\phi_4}{\gamma_0} + \frac{\sigma_6\gamma_0\phi_6}{\alpha_0+\gamma_0}\right) - \\
&\frac{\mu^3\alpha_0\beta}{(\alpha_0+\gamma_0)^3}\left(\frac{\sigma_4\alpha_0\phi_4}{\gamma_0} + \frac{\sigma_6\gamma_0\phi_6}{(\alpha_0+\gamma_0)}\right),
\end{aligned}
\tag{32a}
$$

$$
\begin{aligned}
G = &\left[\mu\left(\frac{\alpha_0^3\beta\gamma_0^2}{(\alpha_0+\gamma_0)}X_1X_2 - \frac{\alpha_0^2\beta\gamma_0^4}{(\alpha_0+\gamma_0)^2}X_2^2\right) + \mu^2\left(-\alpha_0^2\gamma_0^2X_1 + \frac{\alpha_0^2\gamma_0^4}{(\alpha_0+\gamma_0)^2}X_2 - \right.\right. \\
&\frac{\alpha_0^2\beta^2\gamma_0^2}{(\alpha_0+\gamma_0)}X_1^2X_2 - \left.\frac{\alpha_0^2\beta^2\gamma_0^3}{(\alpha_0+\gamma_0)^2}X_1X_2^2\right) + \mu^3\left(\alpha_0^2\beta\gamma_0X_1 - \frac{\alpha_0^2\beta\gamma_0^3}{(\alpha_0+\gamma_0)^2}X_2 + \right. \\
&\frac{\alpha_0^2\beta\gamma_0^2\left(\alpha_0+\mu^2\right)\left(\gamma_0+\mu^2\right)}{(\alpha_0+\gamma_0)}X_1^2 - \frac{3\alpha_0\beta\gamma_0^3}{(\alpha_0+\gamma_0)}X_2^2 - 3\alpha_0\beta\gamma_0^2\left(\alpha_0+\mu^2\right)\left(\gamma_0+\mu^2\right)X_1X_2 + \\
&\left.\left.\frac{\alpha_0^2\beta\gamma_0\left(\alpha_0^2+2\alpha_0\gamma_0+3\gamma_0^2\right)}{(\alpha_0+\gamma_0)^2}X_1X_2\right)\right] / \left[\alpha_0\gamma_0\left(\alpha_0+\mu^2\right)\left(\gamma_0+\mu^2\right)\right] + \sigma_6\phi_6 + \\
&\frac{\mu^2\sigma_4\left(\alpha_0^2+\alpha_0\gamma_0+\gamma_0^2\right)}{\alpha_0\gamma_0\left(\alpha_0+\gamma_0\right)}\phi_4 + \frac{\mu^2\sigma_6\left[\gamma_0^3\left(\alpha_0+\mu^2\right)\left(\gamma_0+\mu^2\right)+\alpha_0\gamma_0\left(\alpha_0+\gamma_0\right)\right]}{\alpha_0\left(\alpha_0+\gamma_0\right)^3}\phi_6 + \\
&\frac{\mu^3\beta}{(\alpha_0+\gamma_0)}\left(\frac{\sigma_4\phi_4}{\gamma_0} + \frac{\sigma_6\gamma_0\phi_6}{(\alpha_0+\gamma_0)^2}\right).
\end{aligned}
\tag{32b}
$$

C Markov simulation for transformed SEIR model

The complete system in the transformed variables has the stable endemic equilibrium at the origin. To bound the dynamics to the first octant, we transform the new variables by using the original properties of $s \geq 0$, $e \geq 0$, and $i \geq 0$, so that

$$
u \leq \frac{\mu^2 N\gamma_0}{\alpha_0\left(\alpha_0+\gamma_0\right)}, \quad -\frac{N\gamma_0\left(\beta\mu^3+\alpha_0{}^2+\gamma_0\alpha_0\right)}{\alpha_0\beta\mu\left(\alpha_0+\gamma_0\right)} \leq v, \quad -\frac{N\mu^2\left(\alpha_0+\gamma_0\right)}{\gamma_0\alpha_0} \leq w. \tag{33}
$$

Therefore, we define the following new variables:

$$
Y_1 = -u + \frac{N\mu^2\gamma_0}{\alpha_0\left(\alpha_0+\gamma_0\right)}, \tag{34a}
$$

$$
Y_2 = v + \frac{N\gamma_0\left(\beta\mu^3+\alpha_0{}^2+\gamma_0\alpha_0\right)}{\alpha_0\beta\mu\left(\alpha_0+\gamma_0\right)}, \tag{34b}
$$

$$
Y_3 = w + \frac{N\mu^2\left(\alpha_0+\gamma_0\right)}{\gamma_0\alpha_0}. \tag{34c}
$$

In these variables, we define evolution relationships similar to Eq. (30). The complete transformed system will evolve in τ the following way:

$$\begin{array}{ll}
\text{transition} & \text{rate} \\
(Y_1+1,Y_2,Y_3) & \frac{\beta\mu}{N}\left(\frac{\gamma_0}{\alpha_0+\gamma_0}Y_2Y_3+Y_1^2\right) \\
(Y_1-1,Y_2,Y_3) & (\alpha_0+\mu^2)Y_1+\frac{\beta\mu}{N}\left(\frac{\gamma_0}{\alpha_0+\gamma_0}Y_1Y_3+Y_1Y_2\right) \\
(Y_1,Y_2+1,Y_3) & \mu^2N+\frac{\beta\mu}{N}\left(\frac{\alpha_0}{(\alpha_0+\gamma_0)}Y_1Y_3+\frac{\alpha_0}{\gamma_0}Y_1Y_2\right) \\
(Y_1,Y_2-1,Y_3) & \alpha_0Y_1+\mu^2Y_2+\frac{\beta\mu}{N}\left(\frac{\alpha_0}{(\alpha_0+\gamma_0)}Y_2Y_3+\frac{\alpha_0}{\gamma_0}{Y_1}^2\right) \\
(Y_1,Y_2,Y_3+1) & (\alpha_0+\gamma_0)Y_1+\frac{\beta\mu}{N}\left(Y_2Y_3+\frac{(\alpha_0+\gamma_0)}{\gamma_0}{Y_1}^2\right) \\
(Y_1,Y_2,Y_3-1) & (\gamma_0+\mu^2)Y_3+\frac{\beta\mu}{N}\left(Y_1Y_3+\frac{(\alpha_0+\gamma_0)}{\gamma_0}Y_1Y_2\right)
\end{array} . \tag{35}$$

References

1. Anderson, R.M., May, R.M.: Infectious Diseases of Humans. Oxford University Press (1991)
2. Arnold, L.: Random Dynamical Systems. Springer-Verlag (1998)
3. Arnold, L., Imkeller, P.: Normal forms for stochastic differential equations. Probab. Theory Rel. **110**, 559–588 (1998)
4. Bailey, N.T.J.: The Mathematical Theory of Infectious Diseases. Charles Griffin, London (1975)
5. Billings, L., Bollt, E.M., Schwartz, I.B.: Phase-space transport of stochastic chaos in population dynamics of virus spread. Phys. Rev. Lett. **88**, 234101 (2002)
6. Billings, L., Schwartz, I.B.: Exciting chaos with noise: unexpected dynamics in epidemic outbreaks. J. Math. Biol. **44**, 31–48 (2002)
7. Bjørnstad, O.N., Finkenstädt, B.F., Grenfell, B.T.: Dynamics of measles epidemics: Estimating scaling. Ecol. Monogr. **72**(2), 169–184 (2002)
8. Boxler, P.: A stochastic version of center manifold theory. Probab. Theory Rel. **83**, 509–545 (1989)
9. Brauer, F., van den Driessche, P., Wu, J. (eds.): Mathematical Epidemiology. Springer-Verlag (2008)
10. Carr, J.: Applications of Centre Manifold Theory. Springer-Verlag (1981)
11. Colizza, V., Barrat, A., Barthelemy, M., Vespignani, A.: The modeling of global epidemics: Stochastic dynamics and predictability. B. Math. Biol. **68**, 1893–1921 (2006)
12. Coullet, P.H., Elphick, C., Tirapegui, E.: Normal form of a Hopf bifurcation with noise. Phys. Lett. A **111**, 277–282 (1985)
13. Doostan, A., Ghanem, R.G., Red-Horse, J.: Stochastic model reduction for chaos representations. Comput. Methods Appl. Mech. Engrg. **196**, 3951–3966 (2007)
14. Dykman, M.I., Schwartz, I.B., Landsman, A.S.: Disease extinction in the presence of random vaccination. Phys. Rev. Lett. **101**, 078101 (2008)
15. Forgoston, E., Schwartz, I.B.: Escape rates in a stochastic environment with multiple scales (2008). Submitted, available at preprint archive: http://arxiv.org/abs/0809.1345
16. Knobloch, E., Wiesenfeld, K.A.: Bifurcations in fluctuating systems: The center-manifold approach. J. Stat. Phys. **33**(3), 611–637 (1983)
17. Marion, G., Renshaw, E., Gibson, G.: Stochastic modelling of environmental variation for biological populations. Theor. Popul. Biol. **57**(3), 197–217 (2000)
18. Mocek, W.T., Rudnicki, R., Voit, E.O.: Approximation of delays in biochemical systems. Math. BioSci. **198**(2), 190–216 (2005)

19. Moreno, Y., Pastor-Satorras, R., Vespignani, A.: Epidemic outbreaks in complex heterogeneous networks. Eur. Phys. J. B **26**(4), 521–529 (2002)
20. Namachchivaya, N.S.: Stochastic bifurcation. Appl. Math. Comput. **38**, 101–159 (1990)
21. Namachchivaya, N.S., Lin, Y.K.: Method of stochastic normal forms. Int. J. Nonlinear Mech. **26**, 931–943 (1991)
22. Nguyen, H.T.H., Rohani, P.: Noise, nonlinearity and seasonality: The epidemics of whooping cough revisited. J. Roy. Soc. Interface **5**(21), 403–413 (2008)
23. Pastor-Satorras, R., Vespignani, A.: Epidemic dynamics and endemic states in complex networks. Phys. Rev. E **63**, 066117 (2001)
24. Rand, D.A., Wilson, H.B.: Chaotic stochasticity - A ubiquitous source of unpredictability in epidemics. P. Roy. Soc. B - Biol. Sci. **246**(1316), 179–184 (1991)
25. Roberts, A.J.: Normal form transforms separate slow and fast modes in stochastic dynamical systems. Physica A **387**(1), 12–38 (2008)
26. Rohani, P., Keeling, M.J., Grenfell, B.T.: The interplay between determinism and stochasticity in childhood diseases. Am. Nat. **159**(5), 469–481 (2002)
27. Schwartz, I., Smith, H.: Infinite subharmonic bifurcations in an SEIR epidemic model. J. Math. Biol. **18**, 233–253 (1983)
28. Schwartz, I.B., Billings, L., Bollt, E.M.: Dynamical epidemic suppression using stochastic prediction and control. Phys. Rev. E **70**, 046220 (2004)
29. Shaw, L.B., Schwartz, I.B.: Fluctuating epidemics on adaptive networks. Phys. Rev. E **77**, 066101 (2008)
30. Stone, L., Olinky, R., Huppert, A.: Seasonal dynamics of recurrent epidemics. Nature **446**, 533–536 (2007)
31. Vazquez, A.: Spreading dynamics on small-world networks with connectivity fluctuations and correlations. Phys. Rev. E **74**, 056101 (2006)
32. Venturi, D., Wan, X., Karniadakis, G.E.: Stochastic low-dimensional modelling of a random laminar wake past a circular cylinder. J. Fluid Mech. **606**, 339–367 (2008)
33. Watts, D.J., Muhamad, R., Medina, D.C., Dodds, P.S.: Multiscale, resurgent epidemics in a hierarchical metapopulation model. P. Natl. Acad. Sci. USA **102**, 11,157–11,162 (2005)